Nature of relaxation processes revealed by the action signals of intensity-modulated light fields

Vladimir Al. Osipov,[1,*] Xiuyin Shang,[1,2] Thorsten Hansen,[3] Tõnu Pullerits,[1] and Khadga Jung Karki[1]
[1]*Chemical Physics, Lund University, Getingevägen 60, 222 41, Lund, Sweden*
[2]*Agricultural University of Hebei, Lingyusi 289, 071001 Baoding, Hebei, China*
[3]*Department of Chemistry, University of Copenhagen, Universitetspaken 5, DK-2100 Copenhagen, Denmark*
(Received 26 July 2016; revised manuscript received 21 September 2016; published 22 November 2016)

We present a generalized theory and experimental results of the action signals induced by the absorption of two photons from two phase-modulated laser beams. In our experiment, the phases of the laser beams are modulated at the frequencies ϕ_1 and ϕ_2, respectively. Their collinear combination leads to the modulation of the total intensity at the frequency $\phi = |\phi_2 - \phi_1|$. The action signals, such as photoluminescence and photocurrent, which result from the absorption of two photons, are isolated at frequencies $m\phi$, $m \in \{0,1,2,\dots\}$. We demonstrate that the ratio of the amplitudes of the secondary ($m = 2$) and the primary ($m = 1$) signals $A_{2\phi} : A_\phi$ is sensitive to the type of relaxation processes in the media. Such sensitivity originates from the cumulative effects of the nonequilibrated state of the matter between the pulses. When the cumulative effects are small, i.e., the relaxation time is much shorter than the laser repetition rate or the laser intensity is high enough to dominate the system behavior, the ratio achieves the reference value of 1 : 4. This ratio decreases monotonically as the relaxation time increases. Our experimental results from fluorescent molecules rhodamine 6G and rubrene support these theoretical findings. In the case of a second-order relaxation process, the ratio changes rapidly with the excitation intensity. When the recombination rate in the second-order process is significantly slower than the repetition rate of the laser, we observe nonmonotonic behavior of the ratio as a function of excitation population at low excitation intensity, and when the recombination rate and the excitation intensity are high, the ratio approaches the value of 1 : 4. We also use the model to determine the value of the recombination rate of charge carriers in a GaP photodiode.

DOI: 10.1103/PhysRevA.94.053845

I. INTRODUCTION

Intensity modulation of continuous laser beams has been commonly used in the measurement of lifetimes of various action signals, such as photoluminescence (PL) [1–3] and photocurrent [4–6]. The intensity-modulation technique can also be implemented with pulsed lasers, wherein the peak intensity of a train of pulses is modulated. One of the advantages of pulsed excitation is that it can induce nonlinear interactions in the media due to the high peak intensity achievable within one pulse. Such modified techniques have been successfully used in multiphoton lifetime imaging [7]. Among a wide variety of methods (electro-optic modulation or reflection from vibrating surfaces) that can be used to modulate the intensity of the laser beams, only a few, such as the interference of two phase-modulated beams in a Mach-Zehnder interferometer [8–10], have been shown to generate a clean modulation (without undesirable sidebands at the multiples of the modulation frequency) of intensity at a single frequency. Single-frequency-modulated light fields have recently been used in phase-synchronous detection of different coherent and incoherent nonlinear signals [10,11]. In a typical experiment [10], two beams, whose phases are modulated at ϕ_1 and ϕ_2, are used to excite PL from a fluorophore. Collinear combination of the two-phase-modulated beams leads to the modulation of the total intensity at the frequency $\phi = |\phi_2 - \phi_1|$.

In a typical light-matter interaction, the absorption of intensity-modulated light modulates the perturbation on the sample. Consequently, the response from the sample, also known as the action signal, is modulated. However, as the response has a finite lifetime, one typically observes a phase lag and demodulation of the action signal relative to the perturbation [1–3]. Conventional techniques use this information to measure the lifetime when the signal decay can be described by a single exponential. If the signal has many exponential decay components, one typically measures the response at multiple modulation frequencies in order to estimate the lifetimes of each decay component [1–3]. In all cases the measurements are carried out at a constant average excitation intensity. On the other hand, the relaxation processes can be nonexponential and their relative contributions can depend on the strength of the perturbation. Investigation of such relaxation processes by the measurement of lifetimes (in both frequency- and time-domain measurements) remains a challenge. Here, we show that the demodulation of the action signal as a function of the excitation intensity (or the strength of perturbation) can be used to discriminate the different relaxation processes. We use the ratio of the action signals at two different frequencies, ϕ and 2ϕ, as the observable and provide a detailed theoretical analysis of the dependence of the ratio on the experimental parameters, such as the excitation intensity, and system parameters, such as the lifetime of the response. In particular, we analyze the response from molecules and semiconductors that are perturbed by two-photon absorption of a train of laser pulses whose peak intensity is modulated at a single frequency, ϕ. The two-photon absorption process perturbs the system at two frequencies, 2ϕ and ϕ, with a well-defined ratio of 1:4 [10]. We show that the ratio $A_{2\phi} : A_\phi$ of the PL signals from molecules is also close to 1:4. In the case of molecules that have long-lived PL with monoexponential decay, the ratio

*Vladimir.Al.Osipov@gmail.com

decreases with the increase in the excitation intensity. On the other hand, if the PL lifetime is very short compared to the time interval between the laser pulses, the ratio does not show significant change. Our experimental results of two-photon PL from rhodamine 6G and rubrene support the theory. Moreover, our results show that the change in the ratio as a function of the excitation intensity shows characteristic features that can be used to distinguish different relaxation processes. We have analyzed the ratio of photocurrent signals from a semiconductor in which the relaxation is a second-order process (nonexponential). We observe that the ratio shows characteristic shape with minima at low excitation intensity. The position of the minima depends on the recombination rate, and we use this information to quantify the recombination of the charge carriers in a GaP photodiode that is excited by two-photon absorption of femtosecond pulses at 800 nm.

II. MATERIALS AND METHODS

A. Theory

To model phase-modulated multiphoton action signals, we assume that the sample comprises an ensemble of two-level systems placed in homogeneous surroundings. Let $P(t)$ be the population in the first excited state S_1 at time t. If the depopulation of S_1 is by a simple stochastic relaxation to the ground state S_0 (Fig. 1), then the rate of change of the population in S_1 is given by

$$\frac{dP(t)}{dt} = -\Gamma P(t) + R(t), \tag{1}$$

where Γ is the rate of relaxation (depopulation) and $R(t)$ is the rate of the $S_0 \rightarrow S_1$ transition due to the interaction with the light of intensity $I(t)$. The model described by Eq. (1) assumes that the intensity of radiation is small [i.e., $R(t)$ is small], such that $P(t) \ll 1$.

If we use an intensity-modulated light at frequency ϕ to excite the sample by linear absorption, then the transition rate is given by

$$R(t) = sI(t) = R(1 + A_I \sin \phi t), \qquad R \equiv sI_0, \tag{2}$$

where s is the absorption cross section (in the units of cm^2/molecule) and I is measured in the units of photons/(s cm^2). The sinusoidal modulation of the transition rate leads to modulation of the excited-state population:

$$P(t) \propto I_0\tau[1 + A_F \sin(\phi t - \Phi)], \tag{3}$$

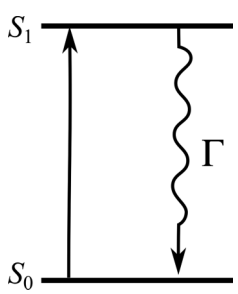

FIG. 1. Diagram of the model of linear absorption in a two-level system.

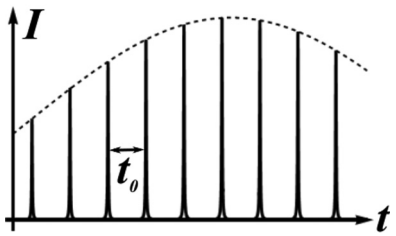

FIG. 2. Intensity of the radiation $I(t)$ is a regular series of δ pulses separated by time intervals t_0. Dashed curve shows the envelope of the pulse intensity.

where τ is the lifetime of the excited state and A_F and Φ are the amplitude and the phase shift of the modulation of the excited-state population, respectively. The modulation of the excited-state population in turn leads to the modulation of the PL; $F(t) \propto P(t)$. Substitution of Eqs. (2) and (3) in Eq. (1) gives [1]

$$\begin{aligned} A_F &= A_I/\sqrt{1+\phi^2\tau^2}, \\ \sin\Phi &= \phi\tau/\sqrt{1+\phi^2\tau^2}, \quad \cos\Phi = 1/\sqrt{1+\phi^2\tau^2}. \end{aligned} \tag{4}$$

In practice, analysis of the signal $F(t)$ is done by Fourier transformation,

$$\begin{aligned} \mathcal{F}[P(t)](\omega) = \frac{1}{2\pi}\int_{-\infty}^{\infty} P(t)\, e^{-i\omega t} dt &= I_0\tau\delta(\omega) \\ &+ \frac{I_0\tau A_F}{2}\delta(\omega-\phi)(\sin\Phi + i\cos\Phi) \\ &+ \frac{I_0\tau A_F}{2}\delta(\omega+\phi)(\sin\Phi - i\cos\Phi). \end{aligned} \tag{5}$$

The value of $\tan\Phi$ can be calculated as a ratio of real and imaginary parts of the amplitude at the peak $\omega = \phi$. The mean square of these amplitudes gives $2A_F$. The Fourier transforms of $P(t)$ and $I(t)$ are connected by the formula

$$\mathcal{F}[P(t)](\omega) = \frac{\tau}{1 - i\omega\tau}\mathcal{F}[I(t)](\omega). \tag{6}$$

Thus, the measurements of the relative phase shift and damping allow us to calculate the lifetime of PL [1–3].

1. Excitation by intensity-modulated light pulses

In this case (see Figs. 1 and 2), the intensity $I(t)$ can be represented by the series

$$I(t) = I_0 \sum_n a_n \delta(t - t_0 n), \tag{7}$$

where $a_n = 1 + A_I \sin(\phi t)$ [see Eq. (2)] and the pulses are approximated by a train of δ-function pulses arriving at time $t_0 n$, where t_0 is the time interval between two consecutive pulses and n is an integer. The modulation frequency ϕ is chosen such that $\phi < 1/t_0$. In what follows, it is convenient to measure all characteristic times of the problem in the scale of

t_0. To this end, we introduce a dimensionless parameter

$$\sigma \equiv t/t_0, \tag{8}$$

such that the pulses arrive at each integer value of σ. We assume that the sample is an ensemble of identical two-level systems placed in homogeneous surroundings. Let $P(\sigma)$ describe the fraction of systems in the excited state S_1. The time evolution of $P(\sigma)$ in our model is given by the kinetic equation

$$\frac{dP(\sigma)}{d\sigma} = -\Gamma P(\sigma) + R[1 - P(\sigma)] \sum_n a_n \delta(\sigma - n),$$
$$P(0) = 0, \tag{9}$$

where $\Gamma = t_0/\tau$. The properties of the δ function allow us to integrate the above equation to obtain the recurrence relation

$$P_n = \gamma P_{n-1} + R_0 a_n (1 - \gamma P_{n-1}), \qquad P_0 = 0,$$
$$\gamma = e^{-\Gamma}, \tag{10}$$

where γ is the fraction of the population that remains in the excited state S_1 after the time interval t_0 and $R_0 = R\Delta t$ (Δt is the pulse duration given by the FWHM of the intensity, and R_0 is the transition probability from the ground state to the excited state). The recurrence relation (10) has a simple physical interpretation: The population P_n of the state S_1 taken at the instance right after the nth pulse, $P_n = P(n + 0)$, is the sum of the population remaining after the $(n - 1)$th pulse reduced by the factor γ and the part of population excited from the ground state S_0. The excitation is proportional to the ground-state population $(1 - \gamma P_{n-1})$ and the amplitude of the pulse a_n taken with the transition probability R_0. The function $P(\sigma)$ has a sawtooth shape, whose analytic expression is

$$P(\sigma) = \sum_{n=0}^{\infty} P_n \Omega_n(\sigma) e^{-\Gamma(\sigma - n)}, \tag{11}$$

where P_n satisfies Eq. (10) subjected to the initial condition $P_0 = 0$ and $\Omega_n(\sigma)$ is an indicator of the time interval $[n, n + 1)$,

$$\Omega_n(\sigma) = \begin{cases} 1, & n \leqslant \sigma < n + 1, \\ 0, & \text{otherwise.} \end{cases} \tag{12}$$

Note that Eq. (9) in comparison with Eq. (1) includes an additional term, $I(\sigma)[1 - P(\sigma)]$, which allows us to take into account the nonequilibrium state of the system between the pulses. We assume that the total number of systems that are excited during the interaction with the pulse is small, i.e., $R_0 \ll 1$, so that the S_0 population is always larger than the S_1 population. Therefore, the light-matter interaction is described by a product of the number of systems in S_0 and the number of photons. In the opposite case of high intensities, i.e., when $R_0 \sim 1$, each light pulse can bleach the ground state S_0, and the second term in the recurrence (10) can get nonphysical negative values. This situation requires a different formulation of the problem that allows the inversion of population in states S_0 and S_1.

Let us first consider the case of time-independent radiation intensity with $a_n = 1$. The solution of Eq. (10) is given by the formula

$$P_n|_{a_n=1} = \frac{R_0}{1 - \gamma + \gamma R_0}[1 - \gamma^n (1 - R_0)^n]. \tag{13}$$

As one can see, the population converges exponentially to the steady-state solution $P_{\text{steady-state}} = R_0(1 - \gamma + \gamma R_0)^{-1}$. When a_n represents some periodic process, the steady state follows the same periodicity. Thus, we can ignore the fast transition to the steady state and start the series in Eq. (11) from $n = -\infty$. By taking the Fourier transform of Eq. (11) using the formula given in Eq. (5), we get

$$\mathcal{F}[P(\sigma)](\omega) = \frac{1}{2\pi} \int_{-\infty}^{\infty} P(\sigma) e^{-i\omega\sigma} d\sigma$$
$$= \frac{1}{2\pi} \sum_{n=-\infty}^{\infty} P_n \int_n^{n+1} e^{-\Gamma(\sigma - n)} e^{-i\omega\sigma} d\sigma$$
$$= \frac{1}{2\pi} \frac{\Gamma - i\omega}{\Gamma^2 + \omega^2} \sum_{n=-\infty}^{\infty} (P_n - \gamma P_{n-1}) e^{-i\omega n}. \tag{14}$$

The sum on the right-hand side represents a Fourier series. PL from molecular systems is proportional to the population of the excited state. Hence, for the time-independent radiation (the case when $a_n = 1$) the PL contains only the dc component, and $\mathcal{F}[P_{\text{steady-state}}](\omega) = R_0(1 - \gamma)(1 - \gamma + \gamma R_0)^{-1}\delta(\omega/\Gamma)$. In the more interesting case, when the pulse intensity is modulated sinusoidally, i.e.,

$$a_n = 1 + A_I \sin(\tilde{\phi} n), \qquad \tilde{\phi} = \phi t_0, \tag{15}$$

and the lifetime is rather short ($\gamma \ll 1$), one can replace the combination $(P_n - \gamma P_{n-1})$ in Eq. (14) by a_n [this follows from the above assumptions and the recurrence equation (10)] to reproduce the results in Eqs. (3), (4), and (5).

In case of finite, but small, γ the form of Eq. (14) allows us to find a general expansion. The recurrence equation (10) together with Eq. (14) yields

$$\mathcal{F}[P(\sigma)](\omega) = \frac{R_0}{2\pi} \frac{\Gamma - i\omega}{\Gamma^2 + \omega^2} \sum_{n=-\infty}^{\infty} [a_n - \gamma R_0 a_n a_{n-1}$$
$$+ \gamma^2 R_0 (R_0 a_n a_{n-1} a_{n-2} - a_n a_{n-2}) + \cdots] e^{-i\omega n}. \tag{16}$$

It is clear that the presence of the term $I(\sigma)[1 - P(\sigma)]$ in the model, Eq. (9), is responsible for the generation of the $a_n a_{n-1} \cdots a_{n-k}$ terms, which describe correlations in the modulated amplitudes. This, in turn, modulates the PL intensity at higher-integer multiples of ϕ.

2. *PL from two-photon absorption of modulated light pulses in a two-level system*

In the case of two-photon absorption (Fig. 3), the rate is proportional to the square of the intensity so that [10]

$$R = s_2 I_0^2, \tag{17}$$

where s_2 is the two-photon absorption cross section and

$$a_n = (1 + \cos \tilde{\phi} n)^2. \tag{18}$$

The steady-state solution of the recurrence equation (10) in the leading order over small $\tilde{\phi}$ is given by

$$P_n = \frac{\beta a_n}{1 + \beta a_n}, \qquad \beta = \frac{\gamma R_0}{1 - \gamma}. \tag{19}$$

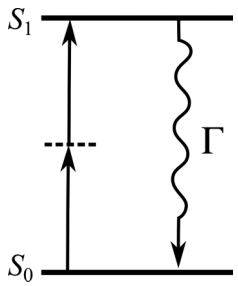

FIG. 3. (a) Diagram of the model of two-photon absorption of the modulated light pulses in a two-level system.

One can calculate also a correction to the steady-state solution, which is given by

$$-\beta\frac{1-R_0a_n}{(1+\beta a_n)^2}\frac{a_n-a_{n-1}}{1-\gamma}+O(\tilde{\phi}^2). \tag{20}$$

The correction becomes essential only if $1-\gamma\sim\beta\tilde{\phi}$, so that the ratio $\frac{\beta(a_n-a_{n-1})}{1-\gamma}$ is finite. For low excitation ($\beta\ll 1$) the correction can be neglected, and the approximation of the steady-state behavior given by Eq. (19) works well.

The PL is proportional to the population of S_1. The Fourier transform of the signal (in the steady-state approximation) is

$$\mathcal{F}[P(\sigma)](\omega)=\frac{R_0(1-\gamma e^{-i\omega})}{2\pi}\frac{\Gamma-i\omega}{\Gamma^2+\omega^2}\sum_{n=-\infty}^{\infty}\frac{a_n}{1+\beta a_n}e^{-i\omega n}. \tag{21}$$

Since the function a_n is periodic and depends only on the exponent $e^{i\tilde{\phi}n}$, the result is a series of δ functions of the form $\delta(\omega-m\tilde{\phi})$, $m=0,\pm1,\pm2,\ldots$. For our purposes (note that we compare the amplitudes only at certain peaks), it is enough to consider only the positive m. When $\beta\ll 1$, one can expand the fraction $\frac{a_n}{1+\beta a_n}$ as a Taylor series in β, which gives

$$\mathcal{F}[P(\sigma)](\omega\sim m\tilde{\phi})=\frac{R_0(1-\gamma e^{-i\omega})}{2\pi}\frac{\Gamma-i\omega}{\Gamma^2+\omega^2}\sum_{n=-\infty}^{\infty}\times\left(a_n-\beta a_n^2+\beta^2a_n^3+\cdots\right)e^{-i\omega n}. \tag{22}$$

The modulation frequencies in the PL intensity calculated by Eq. (22) up to the second order in β yield (only essential terms are presented)

$$\begin{aligned}\mathcal{F}[P(\sigma)](\omega)=&R_0\frac{\Gamma-i\tilde{\phi}}{\Gamma^2+\tilde{\phi}^2}(1-\gamma e^{-i\tilde{\phi}})\left(1-\frac{7}{2}\beta+\frac{99}{8}\beta^2\right)\delta(\omega-\tilde{\phi})+\frac{R_0}{4}\frac{\Gamma-i2\tilde{\phi}}{\Gamma^2+4\tilde{\phi}^2}(1-\gamma e^{-i2\tilde{\phi}})\left(1-7\beta+\frac{495}{16}\beta^2\right)\delta(\omega-2\tilde{\phi})\\&-\frac{R_0\beta}{2}\frac{\Gamma-i3\tilde{\phi}}{\Gamma^2+9\tilde{\phi}^2}(1-\gamma e^{-i3\tilde{\phi}})\left(1-\frac{55}{8}\beta\right)\delta(\omega-3\tilde{\phi})\\&-\frac{R_0\beta}{16}\frac{\Gamma-i4\tilde{\phi}}{\Gamma^2+16\tilde{\phi}^2}(1-\gamma e^{-i4\tilde{\phi}})\left(1-\frac{33}{2}\beta\right)\delta(\omega-4\tilde{\phi})+O(\beta^3)+\cdots.\end{aligned} \tag{23}$$

Thus, the ratios of the amplitudes $A_{m\varphi}$ computed up to the second-order in β are

$$\frac{A_{2\phi}}{A_\phi}=\frac{1}{4}\sqrt{\frac{\Gamma^2+4\tilde{\phi}^2}{\Gamma^2+\tilde{\phi}^2}\frac{1-2\gamma\cos2\tilde{\phi}+\gamma^2}{1-2\gamma\cos\tilde{\phi}+\gamma^2}}\left(1-\frac{7}{2}\beta+\frac{101}{16}\beta^2\right), \tag{24}$$

$$\frac{A_{3\phi}}{A_\phi}=\frac{\beta}{2}\sqrt{\frac{\Gamma^2+9\tilde{\phi}^2}{\Gamma^2+\tilde{\phi}^2}\frac{1-2\gamma\cos3\tilde{\phi}+\gamma^2}{1-2\gamma\cos\tilde{\phi}+\gamma^2}}\left(1-\frac{27}{8}\beta\right), \tag{25}$$

$$\frac{A_{4\phi}}{A_\phi}=\frac{\beta}{16}\sqrt{\frac{\Gamma^2+16\tilde{\phi}^2}{\Gamma^2+\tilde{\phi}^2}\frac{1-2\gamma\cos4\tilde{\phi}+\gamma^2}{1-2\gamma\cos\tilde{\phi}+\gamma^2}}(1-13\beta). \tag{26}$$

In the limiting case when the lifetime of the S_1 state is much shorter than t_0, $\Gamma\gg\tilde{\phi}$ and $\beta\approx 0$, we have $A_{2\phi}:A_\phi\approx 1:4$. In other cases, when β is non-negligible, the ratio $A_{2\phi}:A_\phi$ is smaller than 1:4. Here, also, we note that the finite lifetime of PL ($\beta\neq 0$) gives nonzero amplitudes at frequencies at higher multiples of ϕ.

3. *Photocurrent from two-photon absorption in semiconductors*

The preceding derivations can also be extended to non-exponential relaxation processes, such as the recombination processes in semiconductors. Although there are a number of processes by which the electrons and the holes in a semiconductor can recombine [12], we consider only the simple case of the band-to-band recombination of the charge carriers (Fig. 4). Let $P(t)$ denote the concentration of electrons (holes) in the semiconductor. When the rates of creation and annihilation are in balance at equilibrium, the product of the electron and hole densities remains constant [$P^2(t)=\text{const}$]. The thermal excitation of electrons in a large-band-gap semiconductor is very small, so the corresponding constant is not considered in further analysis. The charge carriers generated by the two-photon absorption result in the increase of electron-hole pairs, and the reverse processes of band-to-band recombination are quadratic in P; thus,

$$\frac{dP(\sigma)}{d\sigma}=-gP^2(\sigma)+R\sum_n a_n\delta(\sigma-n),\quad P(0)=0, \tag{27}$$

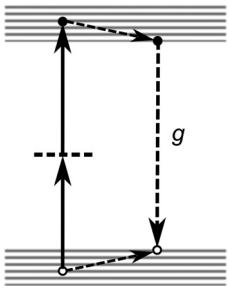

FIG. 4. Model of two-photon absorption of the modulated light pulses in semiconductors.

where g is the recombination rate and R is the transition rate per unit volume. The solution of Eq. (27) is

$$P(\sigma) = \sum_{n=0}^{\infty} \Omega_n(\sigma) \frac{P_n}{1 + g(\sigma - n)P_n}, \tag{28}$$

where P_n satisfy the recurrence

$$P_{n+1} = R_0 a_n + \frac{P_n}{1 + g P_n}. \tag{29}$$

The observable in the experiments is the photocurrent, which is proportional to the number of free carriers generated in the media. The Fourier transform of the observed signal is then given by the formula

$$\mathcal{F}[P(\sigma)](\omega) = \frac{1}{2\pi} \sum_{n=-\infty}^{\infty} e^{-i\omega n} \int_0^1 \frac{P_n}{1 + g\sigma P_n} e^{-i\omega\sigma} d\sigma. \tag{30}$$

When the Fourier transform is calculated in the vicinity of $m\tilde{\phi}$, one can omit the exponent $e^{-i\omega\sigma}$ under the integral to derive $\mathcal{F}[P(\sigma)](\omega \sim m\tilde{\phi}) = \frac{1}{2\pi g} \sum_{n=-\infty}^{\infty} \log(1 + g P_n) e^{-i\omega n}$. The steady-state solution of the recurrence (29) has the form $P_n = \frac{R_0}{2}(a_n + \sqrt{a_n^2 + \frac{4a_n}{g R_0}})$. Its substitution into the above expression leads to a simple expression,

$$\mathcal{F}[P(\sigma)](\omega \sim m\tilde{\phi}) = \frac{1}{2\pi g} \sum_{n=-\infty}^{\infty} \log\left[1 + \mu\left(a_n + \sqrt{a_n^2 + \frac{2a_n}{\mu}}\right)\right] e^{-i\omega n},$$

$$\mu = \frac{g R_0}{2}. \tag{31}$$

As one can see, μ is the main governing parameter of the model. We analyze the behavior of $A_{2\phi} : A_\phi$ at two limiting cases, namely, when $\mu \ll 1$ and $\mu \gg 1$. In the case when $\mu \ll 1$, $\mu(a_n + \sqrt{a_n^2 + \frac{2a_n}{\mu}}) \approx \mu(a_n + \sqrt{a_n}\sqrt{\frac{2}{\mu}}) \leqslant 1$, and the logarithm can be expanded using Taylor's series to obtain the ratio $A_{2\phi} : A_\phi$, which is given by

$$A_{2\phi} : A_\phi = \frac{\mu^{\frac{3}{2}}(112 - 1200\sqrt{2\mu} - \cdots)}{64\sqrt{2} - 80\sqrt{2}\mu + \cdots}. \tag{32}$$

As $\mu \to 0$, the ratio also goes to zero. The ratio shows few oscillations at small values of μ for μ close to zero. Similarly, when $\mu \gg 1$, $\mu(a_n + \sqrt{a_n^2 + \frac{2a_n}{\mu}}) \approx 2\mu a_n$; then the logarithm can be approximated by

$$\log\left[1 + \mu\left(a_n + \sqrt{a_n^2 + \frac{2a_n}{\mu}}\right)\right] \approx \log(2) + \log(\mu) + \log(a_n). \tag{33}$$

In Eq. (33), only the term $\log(a_n)$ contains modulated signal, which can be written as

$$\log(a_n) = \log(2) - \tfrac{1}{4} + \cos(\tilde{\phi}n) - \tfrac{1}{4}\cos(2\tilde{\phi}n) + \cdots. \tag{34}$$

Thus, the ratio of the amplitudes at large values of μ approaches 1:4. Analysis shows that this part of the curve is universal (independent of the choice of ϕ).

B. Experimental setup

The schematic of the optical setup used in the measurements of the two-photon photocurrent from the GaP photodiode is shown in Fig. 5(a). Briefly, a Ti:sapphire oscillator (Synergy from Femtolasers, center wavelength 780 nm, bandwidth 135 nm, repetition rate 70 MHz) was used as the optical source (OS). A pair of chirp mirrors (CMP; Layertec, part number 111298) were used to compensate the group-velocity dispersion induced by the different dispersive optical elements. A 50:50 beam splitter (BS1) was used to split the beam from OS into two identical replicas. The phases of each of the beams were modulated by acousto-optic modulators (AOMs) placed on the arms of a Mach-Zehnder interferometer. The phase modulation frequencies were set to $\phi_1 = 54.7$ MHz and $\phi_2 = 54.75$ MHz, respectively, for AOMs 1 and 2, such that the difference in the phase modulation was $\phi_{21} = 0.05$ MHz. The collinear combination of two phase-modulated beams leads to the modulation of the intensity at ϕ_{21}. It is possible to modulate the intensity by other means, such as an electro-optic modulator; such methods, however, produce undesired sidebands at the multiples of the modulation frequencies. This complicates the analysis.

A piezo-driven retroreflector (DL) in one of the arms of the interferometer was used to adjust the optimal temporal overlap between the two beams. A second beam splitter (BS2) combined the two beams. One of the outputs from BS2 was sent to the microscope, while the other output, which was monitored by a photodiode (PD), served as the reference. We used an inverted microscope (Nikon Ti-S) in the setup. A reflective objective (RO, 36X/0.5 NZ, Edmund Optics) was used to focus the beam onto a gallium phosphide photodiode (Thorlabs, part number FGAP71). The size of the focus spot was about 1.5 μm. The pulse duration Δt at the sample was about 10 fs. The photocurrent from the photodiode was amplified by an amplifier (SR570, Stanford Research Systems), and the output of the amplifier was analyzed by using a generalized lock-in amplifier (GLIA). [13–15]

The schematic of the setup used to measure the two-photon PL from rhodamine 6G in methanol and rubrene in toluene is shown in Fig. 5(b). The two-photon PL from a 10-mM solution was detected in the epidirection using the same microscope objective. A dichroic mirror (DM; FF670-SDi01-25x36) was used to separate the PL from the excitation beam. Another

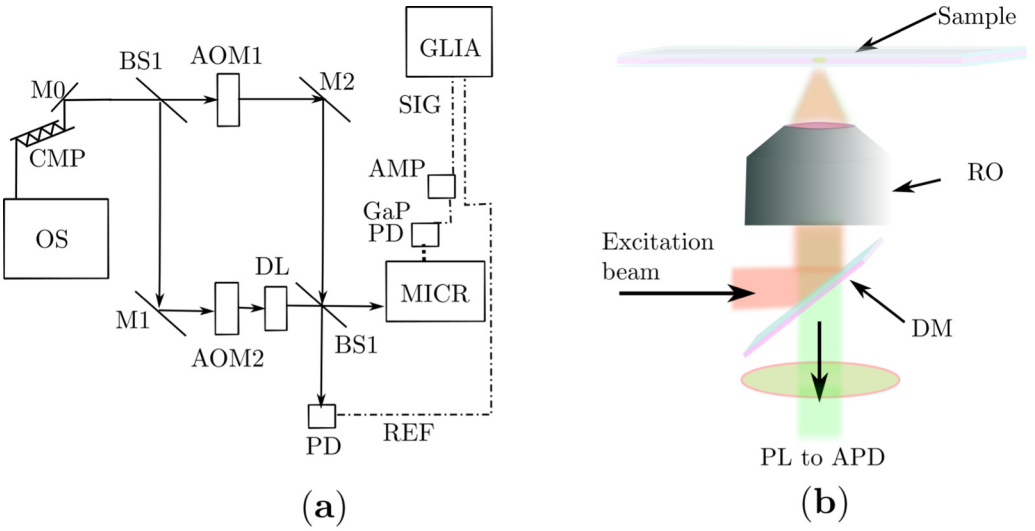

FIG. 5. (a) Schematics of the experimental setup used to measure two-photon photocurrent from a GaP photodiode. OS: mode-locked oscillator, CMP: chirp-mirror pair, M: mirror, BS: beam splitter, AOM: acousto-optic modulator, DL: delay line, PD: photodiode, REF: reference, MICR: microscope (inverted), AMP: current-to-voltage amplifier, SIG: signal, and GLIA: generalized lock-in amplifier. (b) Schematic of focusing optics in a microscope used in excitation and collection of two-photon photoluminescence from rhodamine 6G. DM: dichroic mirror, PL: photoluminescence, APD: avalanche photodiode, RO: reflective objective (Cassegrain).

band pass filter (FIL; 550 × 50 nm, OD 5, Edmund Optics, part number 84772) was used to further suppress the scattered light from reaching the detector. An avalanche photodiode with a bandwidth of 2 MHz (APD; Laser Components, part number LCSA3000-01) was used to detect the PL. As in the case of the photocurrent detection scheme, the final electronic signal from the APD was digitized by a digitizer and analyzed using a generalized lock-in amplifier.

III. RESULTS AND DISCUSSION

A. Two-photon PL from rhodamine 6G

Figure 6(a) shows the ratio of the amplitudes computed by simulating the population of two-level system by using Eqs. (10) and (11) and the Fourier transform of the excited-state population using Eq. (14). In order to compare with the experimental results, we have shown the ratios for $\tau = 4.4$ ns and $\tau = 14.0$ ns. The data are plotted for transition probabilities $R_0 < 0.016$, which correspond to the experimental conditions. t_0 in the simulations is set to 14.3 ns. As can be seen, the ratio decreases slightly but remains close to 1:4 for $\tau = 4.4$ ns. This behavior is well reproduced by the approximate formulas (24)–(26) [Fig. 6(b)].

In Fig. 6(c), we show the experimentally determined ratio of $A_{2\phi} : A_{\phi}$ in rhodamine 6G at different R_0. R_0 is varied by changing the intensity of the laser beams. Under two-photon excitation, the transition probability is given by

$$R_0 = s_2 I_0^2 \Delta t. \tag{35}$$

The molecular two-photon absorption cross section s_2 of rhodamine 6G is about 15×10^{-50} cm^4 s photon^{-1} [16]. At the lowest and the highest excitation intensities, we have pulse energies of 0.034 and 0.136 nJ, respectively. The corresponding transition probabilities are $R_0 = 9.7 \times 10^{-4}$ and 1.55×10^{-2} (transition per pulse), respectively. In our experiments, the lowest excitation intensity is limited by the sensitivity of the detector, and the highest excitation intensity is limited by the maximum available laser power. Note that the maximum $R_0 \ll 1$. The PL lifetime of rhodamine 6G in methanol at 10-mM concentration is about 4.4 ns [17], which is almost 3 times smaller than the time interval between the laser pulses ($t_0 \simeq 14.29$ ns). Under these conditions, $\Gamma \approx 3.24$, $\gamma \approx 0.04$, $\tilde{\phi} = 7.145 \times 10^{-4}$, and $4 \times 10^{-5} \leqslant \beta \leqslant 6.46 \times 10^{-4}$. Using these parameters in Eq. (24), we get $A_{2\phi} : A_{\phi} \approx 1 : 4$ for all the excitation intensities in our measurements, which agrees with the results from the full simulation using Eqs. (10) and (14) and the approximate formula given by Eq. (24). The ratio $A_{2\phi} : A_{\phi}$ obtained from the two-photon PL from rubrene in toluene is shown in Fig. 6(d). The two-photon absorption cross section of rubrene averaged over the wavelength 750–900 nm is about 30×10^{-50} cm^4 s photon^{-1} [18], and the PL lifetime is about 14 ns, which is comparable to t_0. The experimentally measured ratio shows a faster decrease than rhodamine, which agrees with the simulation in Fig. 6(a) and approximate formulas given in Eqs. (24)–(26).

B. Two-photon photocurrent from GaP

We have used the recombination kinetics [Eq. (28)] and the recurrence relation [Eq. (29)] to simulate the concentration of electrons in the conduction band of GaP as a function of time. The photocurrent is proportional to the concentration of the free electrons (or charge carriers). The ratio $A_{2\phi} : A_{\phi}$ in the photocurrent as a function of R_0 and g is shown in Fig. 7(a). The two-photon absorption cross section per unit cell of GaP is about $s_2 \approx 1.2 \times 10^{-48}$ cm^4 s photon^{-1} [19]. The photon fluxes at the lowest and the highest excitation densities we have used in our experiments are 2.2×10^{29} and 2.4×10^{30} photons cm^{-2} s^{-1}, respectively. The corresponding transition probabilities (per laser pulse) for the highest and the lowest excitation densities are 5.8×10^{-4} and 6.9×10^{-2},

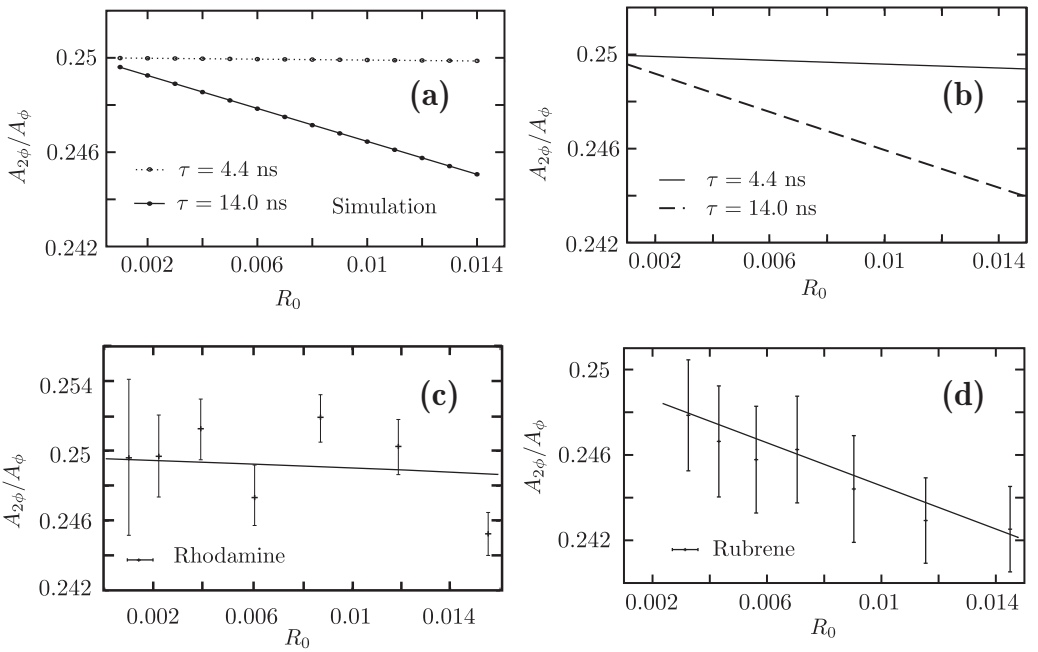

FIG. 6. (a) The ratio of amplitudes $A_\phi : A_{2\phi}$ calculated by formulas (10) and (14) is plotted with respect to R_0 (transition probability) for various τ (lifetime of the excited state). (b) The amplitude ratios $A_{m\phi} : A_\phi$ calculated using the approximate formulas (24), (25), and (26). (c) and (d) The ratio obtained from the measurements of two-photon photoluminescence from rhodamine 6G in methanol and rubrene in toluene, respectively. The modulation frequency ϕ is 50 kHz, and the repetition rate of the laser is about 70 MHz in all the experiments and the simulations.

respectively. Thus, in Fig. 7, we show only the ratio for R_0 that corresponds to the experimental conditions. The ratio calculated from the simulations shows that it is a function of the product $g R_0$, which is in agreement with Eq. (31). In Fig. 7(b), we show the experimentally observed ratio as a function of R_0. The measurements are done by varying the excitation intensity, and the corresponding R_0 are calculated using Eq. (35). As can be seen, the ratio has a minimum at $R_0 = 0.009$. Comparing Figs. 6 and 7, we observe that the first-order and second-order relaxation processes can be distinguished qualitatively simply by the dependence of the ratio on R_0. In a first-order process the ratio decreases monotonically with increasing R_0, while in a second-order process we observe undulations.

Moreover, in a second-order relaxation process, we can accurately estimate the value of recombination g from the position of the minima in Fig. 7(a). For a vertical cut at

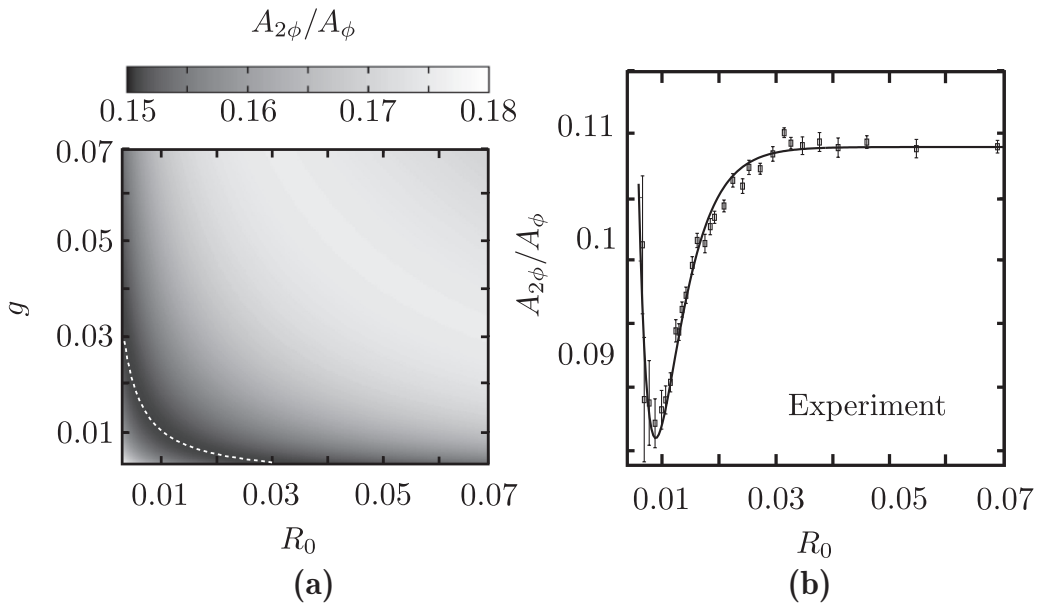

FIG. 7. (a) The ratio of amplitudes $A_\phi : A_{2\phi}$ as a function of g and R_0 obtained from the simulations and (b) the experimentally obtained ratio as a function of R_0 (the points are the data points from the measurements, and the solid line is a spline fit).

$R_0 = 0.009$ in Fig. 7(a), we find minima at $g = 0.013$, which gives the number of recombinations during the interval between the pulses. In the units of recombinations per second, the rate is $g/t_0 \approx 9.1 \times 10^5$ s^{-1}. It is customary to report the recombination parameters in terms of the recombination coefficient, which we calculate as follows. The recombination coefficient is given by $r = g/\rho_c$, where ρ_c is the density of free charge carriers created by the absorption of photons. The energy absorbed during the two-photon excitation process is given by $\Delta E = \Delta I \Delta t \ominus$, where ΔI is the change in the intensity of the light after absorption and $\ominus$ is the area of the focus spot. The change in the intensity can be calculated by the relation $\Delta I = s_2 x I_m^2/(VE)$, where V is the volume of the unit cell of GaP, E is the energy of a single photon, x is twice the Rayleigh length of the beam (confocal parameter), and I_m is the intensity corresponding to $R_0 = 0.009$, i.e., R_0 at the minima. Using the values $s_2 = 1.2 \times 10^{-48}$ cm^4 s photon^{-1}, $V = 1.62 \times 10^{-21}$ cm^3, $x = 4.4 \times 10^{-4}$ cm, $I_m = 2.23 \times 10^{11}$ W cm^{-2}, and $E = 2.48 \times 10^{-19}$ J photon^{-1}, we get $\Delta I = 6.56 \times 10^{10}$ W cm^{-2} and $\Delta E = 11.6 \times 10^{-12}$ J. The number of absorbed photons is $\Delta n = 4.7 \times 10^7$, and the number of generated electron-hole pairs is $n_c = \Delta n/2 = 2.35 \times 10^7$. Then, the density of the free charge carriers is $\rho_c \approx 0.3 \times 10^{19}$ cm^{-3}, which gives the recombination coefficient $r \approx 3 \times 10^{-13}$ cm^3 s^{-1}. The recombination coefficient in GaP measured by using other optical techniques is about 10^{-13} cm^3 s^{-1} [20], which is similar to the value we have obtained.

IV. CONCLUSIONS AND OUTLOOK

We have presented a theoretical analysis of the actions signals such as PL from molecules and photocurrent from semiconductors that are excited by intensity-modulated pulsed lasers. Although it has been widely accepted that the excitation at a fixed modulation frequency ϕ modulates the action signals at the same frequency, our analysis shows that the action signals can have modulations at higher frequencies $n\phi$ if the lifetime of the signals is longer than the repetition rate of the laser [see Eq. (16)]. Our analysis of the two-photon PL shows that the ratio of the signals modulated at 2ϕ and ϕ depends on the excitation intensity. At low excitation intensity, the ratio converges to the previously known values [7], and at higher excitation intensity the ratio decreases. Moreover, when the lifetime of the photoluminescence is short compared to the repetition of the laser, the ratio becomes 1:4, the signature of two-photon absorption. We also show that the intensity dependence of the ratio of the signals at 2ϕ and ϕ can be used to distinguish different relaxation processes. Although the ratio decreases monotonically with increasing intensity for a first-order relaxation process, it shows nonmonotonic behavior in the case of a second-order relaxation process. We have experimentally verified these theoretical predictions. More importantly, we have also shown that the recombination coefficient of free charge carriers in semiconductors can be quantified using the ratio. Our calculations show that the recombination coefficient in a GaP photodiode is about 3×10^{-13} cm^3 s^{-1}.

In this article, we have analyzed only the action signals due to the first- and second-order relaxation processes. Contributions of other higher-order relaxation processes, such as Auger recombination, to the ratio of the signals at 2ϕ and ϕ as a function of the excitation intensity remain to be investigated. Moreover, the ratio could also be sensitive to spatial dynamics of excitations, such as energy transfer, diffusion, and drift of free charges. The analysis we have followed in this article can be generalized to include such processes too.

ACKNOWLEDGMENTS

This work was supported by research grants from the Swedish Research Council (VR), the Crafoord Foundation, NanoLund, the Lundbeck Foundation, and Knut and Allice Wallenberg foundation (KAW).

[1] D. M. Jameson, E. Gratton, and R. D. Hall, The measurement and analysis of heterogeneous emissions by multifrequency phase and modulation fluorometry, Appl. Spectrosc. Rev. **20**, 55 (1984).

[2] T. W. J. Gadella, Jr., T. M. Jovin, and R. M. Clegg, Fluorescence lifetime imaging microscopy (flim): Spatial resolution of microstructures on the nanosecond time scale, Biophys. Chem. **48**, 221 (1993).

[3] J. R. Lakowicz, *Principles of Fluorescence Spectroscopy* (Springer, New York, 2006).

[4] L. Chen, Y. Zhou, S. Jiang, J. Kunze, P. Schmuki, and S. Krause, High resolution LAPS and SPIM, Electrochem. Commun. **12**, 758 (2010).

[5] M. N. Draa, A. S. Hastings, and K. J. Williams, Comparison of photodiode nonlinearity measurement systems, Opt. Express **19**, 12635 (2011).

[6] V. F. Lvovich, *Impedance Spectroscopy: Applications to Electrochemical and Dielectric Phenomena* (Wiley, Hoboken, NJ, 2015).

[7] S. S. Howard, A. Straub, N. G. Horton, D. Kobat, and C. Xu, Frequency-multiplexed in vivo multiphoton phosphorescence lifetime microscopy, Nat. Photonics **7**, 33 (2013).

[8] P. F. Tekavec, T. R. Dyke, and A. H. Marcus, Wave packet interferometry and quantum state reconstruction by acousto-optic modulation, J. Chem. Phys. **125**, 194303 (2006).

[9] K. J. Karki, J. R. Widom, J. Seibt, I. Moody, M. C. Lonergan, T. Pullerits, and A. H. Marcus, Coherent two-dimensional photocurrent spectroscopy in a PbS quantum dot photocell, Nat. Commun. **5**, 5869 (2014).

[10] K. J. Karki, L. Kringle, A. H. Marcus, and T. Pullerits, Phase-synchronous detection of coherent and incoherent nonlinear signals, J. Opt. **18**, 015504 (2015).

[11] L. Bruder, M. Binz, and F. Stienkemeier, Efficient isolation of multiphoton processes and detection of collective resonances in dilute samples, Phys. Rev. A **92**, 053412 (2015).

[12] P. Landsberg, *Recombination in Semiconductors* (Cambridge University Press, Cambridge, 1991).

[13] K. J. Karki, M. Torbjörnsson, J. R. Widom, A. H. Marcus, and T. Pullerits, Digital cavities and their potential applications, J. Instrum. **8**, T05005 (2013).

[14] S. Fu, A. Sakurai, L. Liu, F. Edman, T. Pullerits, V. Öwall, and K. J. Karki, Generalized lock-in amplifier for precision measurement of high frequency signals, Rev. Sci. Instrum. **84**, 115101 (2013).

[15] A. Jin, S. Fu, A. Sakurai, L. Liu, F. Edman, T. Pullerits, V. Öwall, and K. J. Karki, Note: High precision measurements using high frequency gigahertz signals, Rev. Sci. Instrum. **85**, 126102 (2014).

[16] A. Nag and D. Goswami, Solvent effect on two-photon absorption and fluorescence of rhodamine dyes, J. Photochem. Photobiol. A **206**, 188 (2009).

[17] K. A. Selanger, J. Falnes, and T. Sikkeland, Fluorescence lifetime studies of rhodamine 6G in methanol, J. Phys. Chem. **81**, 1960 (1977).

[18] P. Irkhin and I. Biaggio, Two-photon absorption spectroscopy of rubrene single crystals, Phys. Rev. B **89**, 201202 (2014).

[19] I. M. Catalano, A. Cingolani, and A. Minafra, Multiphoton transitions at the direct and indirect band gaps of gallium phosphide, Solid State Commun. **16**, 417 (1975).

[20] A. A. Bergh and P. J. Dean, *Light-Emitting Diodes* (Clarendon, Oxford, 1976).